Chinese Chemical Letters 35 (2024) 108891

Contents lists available at ScienceDirect

Chinese Chemical Letters

journal homepage: www.elsevier.com/locate/cclet

Highly efficient capture of thorium ion by citric acid-modified chitosan gels from aqueous solution

Linshan Peng[a], Qihang Peng[a], Tianxiang Jin[a,b,*], Zhirong Liu[a], Yong Qian[a,*]

[a] State Key Laboratory of Nuclear Resources and Environment, East China University of Technology, Nanchang 330013, China
[b] Jiangxi Province Key Laboratory of Polymer Micro/Nano Manufacturing and Devices, East China University of Technology, Nanchang 330013, China

ARTICLE INFO

Article history:
Received 2 April 2023
Revised 15 July 2023
Accepted 2 August 2023
Available online 5 August 2023

Keywords:
Thorium
Adsorption
Citric acid
Chitosan
DFT calculation

ABSTRACT

A novel citric acid-modified chitosan gel (CSCA) was synthesized through a simple one-step process and was used to extract thorium ions from wastewater. The CSCA samples with varying chemical compositions were analyzed using SEM with mapping EDS, FT-IR, and static water contact angle measurements, and their adsorption behaviors were studied in detail. The results showed that the adsorption performance of CSCA improves with the increase of CA content in the sample. CSCA possesses an impressive capacity for thorium adsorption of 279.8 mg/g. Furthermore, it showed an ultra-fast adsorption rate and reached equilibrium within 30 min. In terms of recyclability, the CSCA still retained more than 86% of its initial adsorption capacity after 6 cycles of reuse. Density functional theory (DFT) analysis reveals that the good selectivity of this material towards thorium ions should be attributed to the high density of adsorption sites and strong interaction between carboxyl groups and thorium ions. This work could be beneficial in the design and synthesis of new polymer materials for extracting thorium.

With the emergence of an energy crisis, the development of sustainable energy has become one of the main challenges confronting contemporary society [1]. Among a range of radioactive elements, thorium-based fuel is seen as a leading contender due to its low cost and high security [2]. Thorium is generally viewed as a very stable element, normally found in the earth's crust incorporated in rare earth minerals such as monazite [3,4]. However, the extraction of pure thorium compounds necessary for nuclear fuel production entails processing thorium-bearing ores, which may potentially result in the release of hazardous thorium-containing wastewater. Consequently, mitigating and minimizing this form of pollution has become an urgent priority. In order to achieve both improved thorium fuel production and environmental protection, an effective method for recovering thorium from aqueous solutions is necessary.

There are many methods for removing harmful metal ions from such solutions, including biological enrichment [5], precipitation [6], and chemical adsorption [7–9]. While biological enrichment is cheap, its removal efficiency is low, so it is rarely employed in practice. Precipitation can yield much higher removal rates, but the sediment produced can be difficult to recover, leading to possible secondary pollution. Chemical adsorption has the benefits of being both cost-effective and environmentally-friendly, making it a widely-used approach.

Chitosan (CS), a cationic polysaccharide in neutral, is obtained from the deacetylation process of chitin [10]. It is similar in structure to cellulose but also possesses amino groups that give it enhanced chemical activity, aiding its use as a functional biomaterial viable for numerous applications. Previous research has demonstrated that raw chitosan performs poorly when used for thorium ion removal, mainly due to the lack of adsorption functional groups [11]. Therefore, modification is necessary to address this issue. Citric acid (CA) is a common organic acid produced on a large scale by fermentation [12] and is well-suited for thorium ion adsorption due to the abundance of carboxyl groups it possesses [11]. Furthermore, the specific mechanism by which adsorption group density influences adsorption efficiency not been fully elucidated. To tackle this challenge, this study synthesized citric acid-modified chitosan (CSCA) with varying carboxyl group densities by regulating the citric acid concentration in the precursor materials. The adsorption performance, isotherms, kinetics, and thermodynamics of thorium(IV) on CSCA with different carboxyl group densities were comprehensively evaluated, and the underlying mechanisms governing thorium(IV) adsorption on CSCA were systematically analyzed.

Structural stability is also critical for the practical application of chitosan. In our previous work [13], we found that using a crosslinking agents composed of multiple components (urea and

* Corresponding authors.
E-mail addresses: 201660027@ecut.edu.cn (T. Jin), yqianecit@163.com (Y. Qian).

https://doi.org/10.1016/j.cclet.2023.108891
1001-8417/

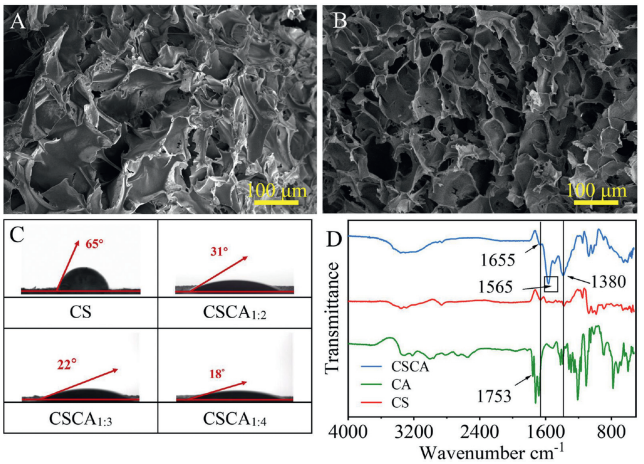

Fig. 1. SEM micrographs of (A) CS and (B) $CSCA_{1:4}$. (C) Contact angle data of CS, $CSCA_{1:2}$, $CSCA_{1:3}$, $CSCA_{1:4}$. (D) FI-IR spectra of CA, CS and CSCA.

phytic acid) could significantly enhance the stability of material structure. However, this crosslinking system requires harsh reaction conditions, including the addition of catalysts and completion of the crosslinking reaction at high temperatures. To address these issues, in this system, we have selected citric acid and glutaraldehyde as crosslinking agents that can form crosslinked structures with chitosan without the need for a catalyst at room temperature [14].

The SEM images of CS and $CSCA_{1:4}$ are shown in Figs. 1A and B, respectively. These images show that the surface morphology of CS becomes looser and has obvious pore structure after CA modification. Elemental distribution mapping of $CSCA_{1:4}$ (Fig. S2 in Supporting information) indicates that the distribution of C, O, N is homogeneous, which demonstrates CA molecules are distributed in CSCA matrix. The element composition of different samples, as tested by SEM-EDS, is detailed in Fig. S2 and Table S1 (Supporting information). As seen, increasing CA content resulted in a decrease in the proportion of carbon and nitrogen in the material, and an increased proportion of oxygen. The above data manifest that the CA content increases gradually from CS to $CSCA_{1:4}$, and that the element composition of $CSCA_{1:3}$ and $CSCA_{1:4}$ is almost unchanged, indicating that the content of CA groups was close to saturation when the mass ratio of CS to CA was 1:3.

Furthermore, the results from water contact angle measurements (Fig. 1C) showed that the water contact angles of CS, $CSCA_{1:2}$, $CSCA_{1:3}$ and $CSCA_{1:4}$ were 65°, 31°, 22°, and 18°, respectively. Citric acid is a strong acid that can be ionized in water, so the modification of citric acid will significantly improve the hydrophilicity of chitosan. Therefore, the improvement of the above hydrophilic properties proves that the CA content in samples increases from CS to $CSCA_{1:4}$, which is consistent with the experimental results of water contact angle. The porous structure and excellent hydrophilicity can promote the diffusion rate of water molecules and ions in gel materials, thereby improving the adsorption efficiency of thorium ions.

FT-IR is used to analyze the chemical structure of different samples, and the results are shown in Fig. 1D. The peak at 1080 cm^{-1} corresponds to C–O–C, which is one of the characteristic peaks of chitosan, and can be observed in both CS and CSCA [15]. For the CSCA sample, an obvious new peak appeared at 1565 cm^{-1}, which is attributed to the absorption of amide II band. This phenomenon indicates that there is an amidation reaction between CA and CS [14]. The absorption peaks of carboxyl group in both CS and CSCA appear at 1380 cm^{-1}. The intensity of carboxyl group peak in CSCA is significantly higher than that in CS, indicating that more carboxyl groups appear on CS through the modification of CA [16]. A peak of carboxyl at 1753 cm^{-1} can be observed to be significantly weakened in CSCA, indicating that the carboxyl in citric acid has participated in the reaction [17]. For CS, the broad absorption peak in the range of 3200–2500 cm^{-1} is the stretching vibration peak of O–H. This peak is enhanced in CSCA, indicating that intermolecular hydrogen bonds are formed between CA and CS.

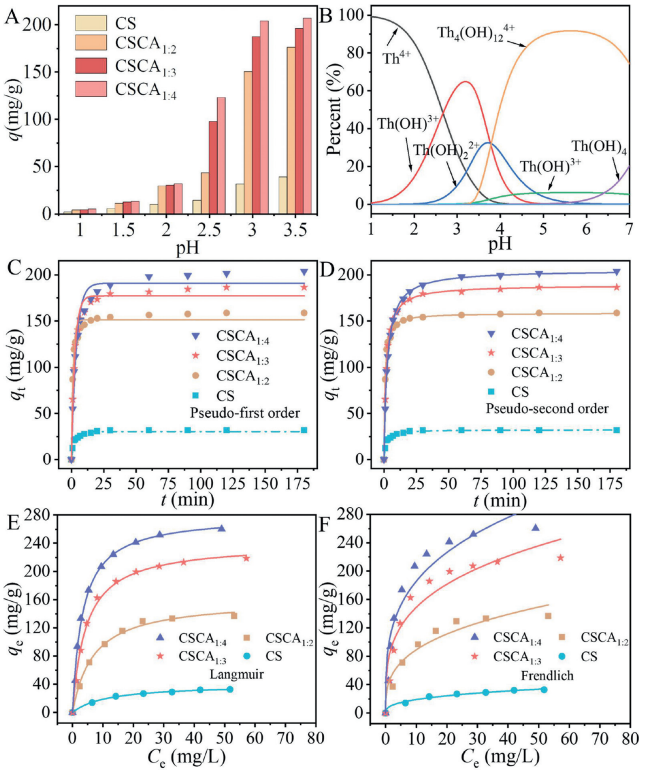

Fig. 2. (A) The effect of pH on the adsorption of Th(IV) onto CS, $CSCA_{1:2}$, $CSCA_{1:3}$ and $CSCA_{1:4}$ ($m = 5$ mg, $C_0 = 50$ mg/L, $t = 180$ min, $T = 298.15$ K). (B) Distribution of Th(IV) species at different pH values with a total concentration of 50 mg/L. Adsorption kinetics of Th(IV) onto different samples and fitting curves of the pseudo-first order dynamic equation (C) and the pseudo-second order dynamic (D) (pH = 3.0, $m = 5$ mg, $V = 25$ mL, $C_{Th} = 50$ mg/L, $T = 298.15$ K). (E) Langmuir and (F) Freundlich isotherm models for adsorption of Th(IV) onto different samples (pH = 3.0, $m = 5$ mg, $V = 25$ mL, $C_{Th} = 50$ mg/L, $T = 298.15$ K).

As shown in Fig. 2A, the adsorption capacities of all samples increase as pH increases. Moreover, at any pH value, the adsorption capacity of $CSCA_{1:4}$ is comparatively higher than those of other samples. This phenomenon could be attributed to the oxygen-containing groups (COOH) provided by CA that effectively establishes strong complexation with Th(IV) [18]. In order to further determine the optimal pH of thorium ion adsorption, we used Visual MINTEQ 3.1 software to simulate the distribution of Th(IV) in aqueous solution under different pH values. As shown in Fig. 2B, when pH < 3.0, Th(IV) mainly exists in the forms of Th^{4+} and $Th(OH)^{3+}$. When pH continues to increase from 3.0, the concentration of $Th(OH)_2{}^{2+}$ increases significantly, which will significantly affect the adsorption process of Th on CSCA. In view of the above, we set the most suitable pH at 3.0. The effect of ionic strength on Th(IV) adsorption of CS and $CSCA_{1:4}$ was shown in Fig. S3 (Supporting information). As the concentration of sodium chloride increases, the adsorption efficiency of CS and $CSCA_{1:4}$ decreased slightly. This phenomenon was attributed to the higher probability of Na^+ occupying the active sites for separation due to the increased ionic strength [18].

The relationship between sorption amount and contact time in the Th(IV) sorption of CS and CSCA is shown in Figs. 2C and D.

The sorption equilibrium of Th(IV) by CS and CSCA samples was reached within 30 min. For CS, the adsorption equilibrium could even be attained in 20 min due to its low adsorption capacity. This excellent adsorption efficiency should be attributed to the porous structure and high hydrophilicity of these materials. The kinetic profiles of these samples were simulated with pseudo-first and pseudo-second-order models and the results were shown in Figs. 2C and D and Table S2 (Supporting information). It is revealed from the data that all the sorption processes of these samples were better fitted by the pseudo-second-order model, as evidenced by the relatively higher R^2 value and more accurate calculated q_e, indicating that chemical adsorption should be the rate-controlling step for the sorption of CSCA [19].

Adsorption isotherms were investigated by equilibrating 5 mg of adsorbent separately with various concentrations of Th(IV) solution between 10 mg/L and 60 mg/L (solution volume $V = 25$ mL, pH = 3.0, adsorption time $t = 3$ h). The fitting results (Langmuir and Freundlich model) are shown in Figs. 2E and F and the obtained parameter values are listed in the Table S3 (Supporting information). Results showed that Langmuir model gave higher correlation coefficients (R^2) in comparison with Freundlich model for both CSCA and CS samples, indicating that the adsorption process followed the Langmuir model and formed a monolayer coverage [20]. For $CSCA_{1:4}$, the maximum theoretical adsorption capacity of determined by Langmuir model was 279.8 mg/g, implying that this material has a promising adsorption performance. As presented in Table S4 (Supporting information), $CSCA_{1:4}$ displays a higher maximum capacity than the other adsorbents such as carbon and silica-based materials. Moreover, it can be observed from Langmuir fitting of these four samples that the maximum adsorption capacity of CS was much lower than those of CSCA samples, and the maximum adsorption capacity increased with an increase in the CA content. This strongly suggests that CA acts as an active adsorption site during the process. Furthermore, the relatively small increase in adsorption capacity from $CSCA_{1:3}$ to $CSCA_{1:4}$ could be due to the fact that the amount of CA grafted on chitosan in $CSCA_{1:3}$ is close to saturation, while the amount of CA added in $CSCA_{1:4}$ has been excessive.

Studying the effect of temperature on the adsorption behavior of CSCA is critical for a comprehensive understanding of the adsorption mechanism. The $\ln K_d$ *vs.* $1/T$ graph is presented in Fig. S4 (Supporting information), along with the thermodynamic parameters in Table S5 (Supporting information). $\Delta H_0 > 0$ denotes an endothermic reaction occurring in the process of adsorption. $\Delta S_0 > 0$ implies that the disorder of the system increases during the adsorption process. The increase in the degree of system disorder is mainly attributed to two reasons. Firstly, the random arrangement of adsorption groups and molecular conformational changes can introduce irregularity and complexity within the system, thus limiting the reduction of entropy. Secondly, the destruction of hydration shells of Th(IV) will further increase the entropy of the system [21]. Moreover, since $\Delta G_0 < 0$ at all three temperatures tested, it indicates that the adsorption process is spontaneous under these temperatures, and the capacity of adsorption increases as the temperature increases [22].

The reusability of CSCA was investigated by the adsorption-desorption experiment. In this study, the samples were eluted with HCl (0.1 mol/L) for 150 min for desorption after the adsorption process, then it was wash with deionized water for several times to further remove thorium ions adsorbed in the material. HCl solution can wash out adsorbed Th(IV) ions through ion exchange mechanism. Specifically, when the concentration of HCl in the solution increases, H^+ exchanges with cations on the adsorbent material, causing the adsorbed ions to detach from the surface of the material. Fig. S5 (Supporting information) illustrates that a 0.1 mol/L HCl solution can release over 95% of the adsorbed Th(IV) ions. However, increasing the concentration of HCl further did not significantly improve the elution efficiency, and may even cause degradation of the material in acidic environments. Therefore, 0.1 mol/L of HCl solution was used as the desorption agent in desorption experiment.

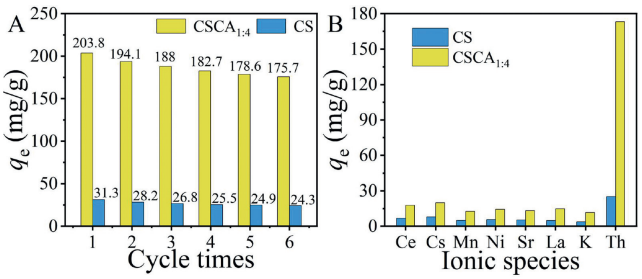

Fig. 3. (A) Th(IV) adsorption capacities of CS and CSCA during the 6 cycles (pH = 3.0, $C_0 = 50$ mg/L, $T = 298.15$ K), (B) Th(IV) adsorption capacities of CS and CSCA with co-existed ions (pH = 3.0, $C_{\text{other ions}} = 0.5$ mol/L, $T = 298.15$ K).

The adsorption capacities of $CSCA_{1:4}$ and CS were shown in Fig. 3A. After six adsorption-desorption cycles, the adsorption capacity of $CSCA_{1:4}$ remained 86.2% of the initial value of its adsorption capacity. There are two reasons for the decrease in adsorption capacity: Firstly, due to the strong interaction between the adsorbed groups in the CSCA material and Th ions, some Th ions will occupy the adsorption active sites and are difficult to elute, which reduces the adsorption capacity. Secondly, during the process of washing with hydrochloric acid, citric acid may be eluted and lost. Comparatively, the adsorption capacity of CS was only about 77.6% of the initial capacity, which indicated that the introduction of CA can significantly improve the recycling performance of CS. This is because there is only a chemical cross-linking structure formed by the reaction of glutaraldehyde and chitosan in CS, but there is not only a chemical cross-linking structure in CSCA, but also a physical cross-linking network formed by the hydrogen bond between CA and chitosan matrix. This structure effectively increases the chemical structure stability of CSCA, thus improving its reusability in acidic environment.

Adsorption selectivity is an important property of materials in practical applications. The effect of interfering ions on Th(IV) adsorption of CSCA was studied. The adsorption experiment was conducted in a multi-component system, and all concentration of the competing ions was 0.5 mmol/L, solid-liquid ratio was 0.25 g/L, and the pH of the solution was 3 ($C_{\text{all}} = 0.5$ mmol/L, pH = 3.0, solid-liquid ratio = 0.25 g/L). As shown in Fig. 3B, the adsorption capacities of both CS and $CSCA_{1:4}$ were decreased compared with the adsorption capacities tested with no interfering ion existed. This is because these ions competed with Th(IV) for binding on the adsorbent surface. However, it can be seen from the results that CSCA had a much higher adsorption capacity for thorium compared to other competing ions, as well as higher selectivity than CS. The remarkable selectivity of CSCA towards Th ions can be attributed to two factors: Firstly, Th ion carries a relatively higher number of positive charges compared to other competing ions, resulting in a stronger Coulomb interaction between Th and the adsorption groups [23]. Secondly, the configuration of CSCA is conducive to the formation of a stable coordination structure between the adsorption groups and Th ions [18].

The XPS spectra of CSCA shown in Fig. 4A exhibits only C 1s, O 1s and N 1s signals. However, two distinct peaks were evident at 340 eV after Th(IV) adsorption, indicating the presence of Th 4f. Further, the high resolution XPS spectra of Th 4f (Fig. 4B) revealed two sharp peaks of 335.0 and 344.2 eV, which correspond to Th $4f_{7/2}$ and Th $4f_{5/2}$, respectively. Moreover, the N 1s spectrum of CSCA before adsorption (Fig. 4C) presented two peaks at 399.0 and

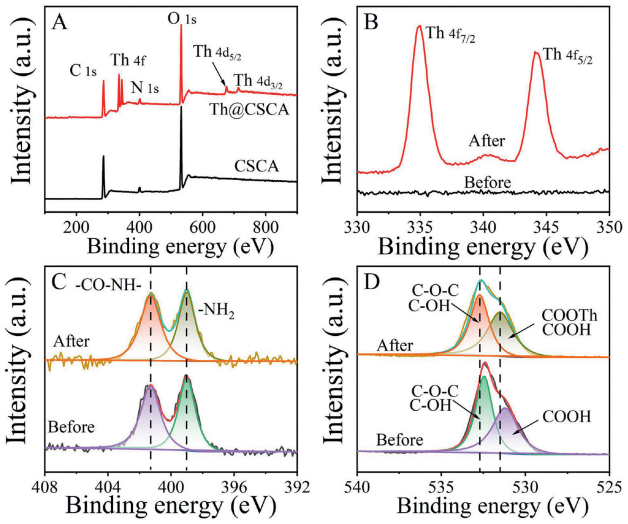

Fig. 4. XPS spectra of CSCA (A) and high-resolution XPS spectra of Th 4f (B), N 1s (C), and O 1s (D) before and after Th(IV) adsorption.

401.3 eV associated with the -NH_2 and –CO–NH– signals, respectively. These peaks did not shift significantly upon Th(IV) adsorption, thus implying that the interaction between these groups and thorium ions is weak. The O 1s spectrum of CSCA (Fig. 4D) was composed of two deconvoluted peaks at 532.4 and 531.2 eV, associated with the C-OH/C-O-C and the COOH groups in CSCA, respectively. Subsequent Th(IV) adsorption resulted in a slight shift in the binding energies of these groups from 532.4 eV to 532.7 eV (C-OH and C-O-C), and 531.2 eV to 531.5 eV (COOH), thereby exhibiting the involvement of C-OH, C-O-C and COOH groups in Th(IV) complexation.

The density function theory (DFT) calculations were used to further study the interaction mechanism between thorium ion and CSCA. The Th(IV) in aqueous solution were modeled by formation of thorium hexahydrate $[Th(H_2O)_6]^{4+}$ according to a previous report [24], as shown in Fig. 5A. The optimized structure shows that Th(IV) was surrounded six water molecule, and there was about 2.476 Å distance between Th and oxygen atoms of water. Subsequently, Th(IV) adsorption on synthetic materials was verified. In our calculations, we carried out an exchange mechanism, which replace the coordinated water molecules in $Th(H_2O)_6^{4+}$ by functional groups of synthetic adsorbent. According to experimental results, the three kinds of groups in synthetic materials were considered. Firstly, the configuration of Th(IV) binding with -NH_2 group (Th-NH_2) was optimized as shown in Fig. 5B. The thorium ion bound NH_2 group by replacing one water molecule of $Th(H_2O)_6^{4+}$, and the bind distance between Th ion and N atom was 2.746 Å. This result indicates that weak interaction between Th ion and amino cyclohexanol. Subsequently, the configuration of Th(IV) binding with C=O ligand on amide group was optimized as shown in Fig. 5C (Th-OCNH). From Fig. 5C, the thorium ion can bind C = O group by replacing one water molecule in thorium hexahydrate. The optimized binding distance between Th ion and C=O group was 2.137 Å. Finally, two possible configuration 1:1 and 1:2 ratio of Th^{4+}synthetic adsorbent were considered in Th-$(COOH)_2$ and Th-$(COOH)_4$ (Figs. 5D and E). As shown in Figs. 5D and E, the thorium ion adsorbed on synthetic materials by C=O groups of polymers, and the simulated bond distance were 2.221 Å and 2.262 Å as well as 2.274 Å, respectively. Generally, the shorter binding distance exhibits stronger interactions. Therefore, we think that Th(IV) was more easily interacted with C = O ligand instead of NH_2 group in polymer, which is consistent with experimental results. Furthermore, these features were confirmed by deformation charge density shown in blue dotted box. It was found that charge accumulation and depletion exist between Th(IV) and C=O groups.

For exchange reactions of $[Th(H_2O)_6]^{4+}$with polymer, the binding reactions free energies (ΔG) were computed by Eq. 1:

$$CSCA + [Th(H_2O)_6]^{4+} \rightarrow Th(H_2O)_{6\text{-}n}{}^{4+} / \ CSCA + nH_2O \quad (1)$$

The calculated ΔG values were negative, indicating that the above binding reactions can be conducted. After corrections by frequency calculation of configurations, the calculated ΔG for formation of Th-OCNH, Th-$(COOH)_2$ and Th-$(COOH)_4$ in exchange reactions were −4.92, −5.38 and −8.16 kcal/mol, respectively. However, the calculated ΔG was 0.74 kcal/mol in Th-NH_2. This result indicates that the exchange reaction can proceed spontaneously proceed in the Th-OCNH, Th-$(COOH)_2$ and Th-$(COOH)_4$, which also confirm thermodynamic results in experimental. According to the above ΔG, adding C=O functional group in synthetic polymers will contribute to the increase of adsorption process. The natural bond orbitals (NBO) [25] analysis for $[Th(H_2O)_6]^{4+}$, Th-OCNH, Th-$(COOH)_2$ and Th-$(COOH)_4$ were also presented. The calculated average WBIs of Th-O (Table S6 in Supporting information) in Th-$(COOH)_4$ (0.394) are higher than those of $[Th(H_2O)_6]^{4+}$ (0.229), Th-

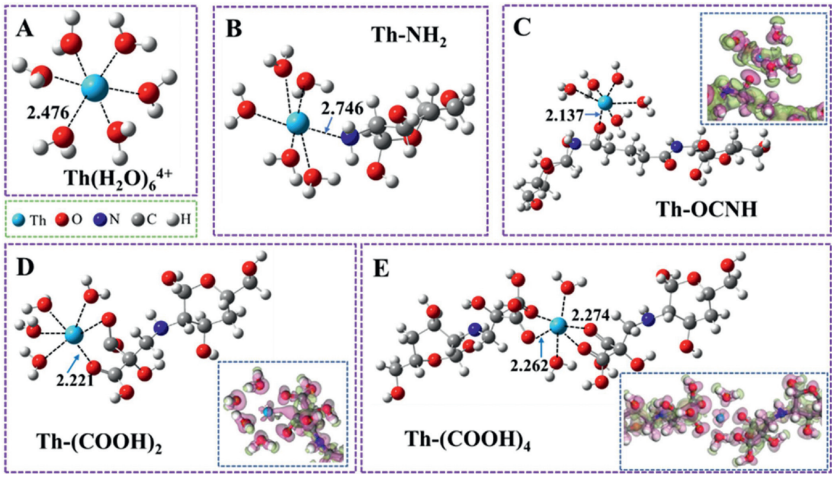

Fig. 5. The optimized configurations of (A) thorium hexahydrate $[Th(H_2O)_6]^{4+}$, (B) 1:1 ratio of Th(IV) with -NH_2 ligand on amino group, (C) 1:1 ratio of Th(IV) with C=O ligand on amide group, (D) 1:2 ratio of Th(IV) with C=O ligands on the same CSCA chain, and (E) 1:4 ratio of Th(IV) with C=O ligands on two distinct CSCA chains. The deformation charge density (binding region between Th(IV) and synthetic adsorbent) was shown in blue dotted box.

OCNH (0.301) and Th-$(COOH)_2$ (0.346). Therefore, the formation of Th-$(COOH)_4$ was more easily and stable during exchange reactions, which makes it highly selective for thorium ion. The removal mechanism diagram of Th(IV) by CSCA was shown in Fig. S6 (Supporting information).

The separation and enrichment of thorium is an important research direction in energy and environmental science. In this work, we synthesized citric acid-modified chitosan gel *via* a one-step method and used it for thorium ion adsorption. Our experimental results showed that when the mass ratio of citric acid to chitosan was 1:4, the citric acid groups in the chitosan reached saturation, and the material ($CSCA_{1:4}$) demonstrated the highest adsorption capacity of 279.8 mg/g. CSCA showed excellent efficiency for adsorbing thorium ions, which can be attributed to its porous structure and good hydrophilicity due to the presence of citric acid groups. Furthermore, CSCA showed a high degree of selectivity for Th(IV) ions, even in the presence of other coexisting metal ions. According to the DFT calculation results, the selective adsorption performance of CSCA is due to the strong binding force of carboxyl functional group with thorium ion. It is noteworthy that the higher the density of carboxyl groups in the material, the stronger the selectivity to thorium ion. All these remarkable adsorption characteristics demonstrate that CSCA is an effective material for thorium ion adsorption.

Declaration of competing interest

The authors declare that they have no known competing financial interests or personal relationships that could have appeared to influence the work reported in this paper.

Acknowledgments

The authors are grateful for the financial support of the Natural Science Foundation of Jiangxi Province (No. 20202BABL213011), the Training Program for Academic and Technical Leaders of Major Disciplines of Jiangxi Province (No. 20225BCJ22008) and the Opening Project of Jiangxi Province Key Laboratory of Polymer Micro/Nano Manufacturing and Devices (No. PMND202201).

Supplementary materials

Supplementary material associated with this article can be found, in the online version, at doi:10.1016/j.cclet.2023.108891.

References

[1] S. Chu, Y. Cui, N. Liu, Nat. Mater. 16 (2017) 16–22.
[2] U.E. Humphrey, M.U. Khandaker, Renew. Sustain. Energy Rev. 97 (2018) 259–275.
[3] H. Nisbet, A.A. Migdisov, A.E. Williams-Jones, et al., Geochim. Cosmochim. Acta 330 (2022) 80–92.
[4] E. Kim, K. Osseo-Asare, Hydrometallurgy 113-114 (2012) 67–78.
[5] C. Wei, X. Cheng, W. Sun, et al., J. Clean. Prod. 411 (2023) 137334.
[6] D. Mendil, M. Karatas, M. Tuzen, Food Chem. 177 (2015) 320–324.
[7] J. Huang, B. Huang, T. Jin, et al., Sep. Purif. Technol. 284 (2022) 120284.
[8] J. Huang, Z. Liu, D. Huang, T. Jin, Y. Qian, Chin.Chem. Lett. 33 (2022) 3762–3766.
[9] J. Huang, Z. Liu, D. Huang, T. Jin, Y. Qian, J. Hazard. Mater. 433 (2022) 128775.
[10] E.M.A. Hejjaji, A.M. Smith, G.A. Morris, Int. J. Biol. Macromol. 95 (2017) 564–573.
[11] Y. Hu, J. Ding, G. Ren, Sep. Purif. Technol. 303 (2022) 122188.
[12] M.Y. Lu, I.S. Maddox, J.D. Brooks, Bioresour. Technol. 54 (1995) 235–239.
[13] T. Jin, Q. Luo, H. Yu, et al., Sep. Purif. Technol. 312 (2023) 123367.
[14] B. Wei, J. Zou, Q. Pu, et al., J. Sci. Food. Agric. 102 (2022) 3826–3834.
[15] C. Niu, N. Zhang, C. Hu, et al., Carbohyd. Polym. 258 (2021) 117644.
[16] N.V. Suc, H.T.Y. Ly, J. Chem. Technol. Biotechnol. 88 (2013) 1641–1649.
[17] Y. Li, Z. Wang, X. Wang, et al., Carbohyd. Polym. 269 (2021) 118269.
[18] L. Hadjittofi, I. Pashalidis, Desalin. Water Treat. 57 (2016) 1–5.
[19] H. Ding, X. Zhang, H. Yang, et al., Chem. Eng. J. 368 (2019) 37–50.
[20] Y. Wang, X. Chen, X. Hu, et al., Appl. Surf. Sci. 536 (2021) 147829.
[21] S. Li, L. Wang, J. Peng, M. Peng, W. Shi, Chem. Eng. J. 366 (2019) 192–199.
[22] T.S. Anirudhan, P.S. Suchithra, P. Senan, A.R. Tharun, Ind. Eng. Chem. Res. 51 (2012) 4825–4836.
[23] W.D. Wang, Y.X. Cui, L.K. Zhang, et al., Int. J. Environ. Sci. Technol. 18 (2020) 2733–2746.
[24] Z. Liang, A.G. Marshall, J. Marcalo, et al., Organometallics 10 (1991) 2794–2797.
[25] A.E. Reed, F.J. Weinhold, Chem. Phys. 78 (1983) 4066–4073.